EasyChair Preprint

№ 5352

Forced Convection Heat Transfer from a Rotating Elliptic Cylinder in the Laminar Flow Regime

Deepak Kumar and Akhilesh Kumar Sahu

EasyChair preprints are intended for rapid dissemination of research results and are integrated with the rest of EasyChair.

April 18, 2021

Proceedings of the 25th National and 3rd International ISHMT-ASTFE Heat and Mass Transfer Conference (IHMTC-2019), December 28-31, 2019, IIT Roorkee, Roorkee, India.

IHMTC2019-xx-xxxx

Forced convection Heat Transfer from a Rotating Elliptic Cylinder in the Laminar Flow Regime

Deepak Kumar and Akhilesh Kumar Sahu*

Department of Chemical Engineering, NIT Rourkela
* Corresponding author email: sahuak@nitrkl.ac.in

ABSTRACT

In this paper numerical investigation has been done to study the forced convection heat transfer from a uniformly heated elliptic cylinder of aspect ratio (e *=0.1*), rotating in anticlockwise direction on its axis with the constant rotational speed in a steady laminar flow regime. The geometry and mesh for the problem is created by commercial software ANSYS 15 and, the governing differential equations for this problem have been solved numerically by using finite volume method based CFD solver FLUENT. In order to capture the transient behaviour of the flow due to the rotation of the elliptic cylinder, the sliding mesh method is implemented, whereby the governing equations are solved using an arbitrary Lagrangian-Eulerian approach. In the present study, the emphasis has been given to see the effect of the Prandtl number which is varying from ($0.7 \leq Pr \leq 100$) and Reynolds number ($5 \leq Re \leq 40$) on the average Nusselt Number (*Nu*), local Nusselt number and comprehensive temperature field. It is found from the investigation that, at constant Prandtl number, the average Nusselt number linearly increases with increment in Reynolds number, and keeping the Reynolds number constant, Nusselt number also increases with increment in Prandtl number. The isotherms profile shown in this paper suggest that with increment in Pr number, and keeping the Re number constant, the thermal boundary layer becomes thinner in the rear side of the cylinder which leads to increase in local Nusselt number and temperature gradient. The detailed streamlines and isotherms patterns are also presented for the range of the conditions.

Keywords: Rotating elliptic cylinder, Heat Transfer, Nusselt Number, Prandtl number, Rotation rate

NOMENCLATURE

C_P= heat capacity, $J/Kg\ K$

a = semi major axis of the elliptical cylinder, m

b = semi minor axis of the elliptical cylinder, m

e = aspect ratio of an elliptical cylinder, $(= {}^{b}/_{a})$

h = heat transfer coefficient, W/m^2K

k = thermal conductivity of the fluid, $W/m\ K$

Nu = surface average Nusselt number, dimensionless

Nu_L = local Nusselt number, dimensionless

Pr = Prandtl number, dimensionless

$Re =$ Reynolds number, dimensionless

P = non – dimensional pressure

p = pressure, Pa

ρ = density of fluid, Kg/m^3

T_∞ = temperature of fluid at inlet, K

T_w = temperature at the surface of the cylinder, K

T = temperature of the fluid, K

T^* = non-dimensional temperature

u, v = velocity in x and y-direction respectively, m/s

u_∞ = freestream velocity of the fluid at the inlet, m/s

U = non-dimensional velocity in x-direction

V = non-dimensional velocity in y-direction

x = streamwise coordinate, m

y = transverse coordinate, m

X = non-dimensional streamwise coordinate

Y = non-dimensional transverse coordinate

t = time, s

τ = non – dimensional time

θ = angular displacement from the front stagnation point

α = non-dimensional rotational velocity $(= {}^{a\omega}/_{u_\infty})$

ω = angular velocity of cylinder rotation, rad/s

μ = viscosity, $Pa.s$

INTRODUCTION

Heat transfer from rotating cylinder has been a topic of great attention for academics due to its application in numerous engineering practices such as heat exchange from rotatory machinery, solar energy system, cylindrical cooling devices in chemical processing and food processing industries. The available research work on fluid flow and heat transfer around an object is mainly focused on the rotating and non-rotating circular cylinder [1- 4]. Its elliptical counterpart can also be seen in process industry but is not studied up to the same extent. An elliptic cylinder in general form can be a flat plate and also a circular cylinder depending upon the ratio of the minor axis to the major axis of the cylinder. Various researchers [5-7] have shown that the mean heat transfer rate from the elliptical cylinder is higher than that from the circular cylinder. They also reveal that the local heat transfer behaviour at the surface of the elliptical cylinder is quite different from that of a circular cylinder, and the average Nusselt number depends on Reynolds number along with the angle of attack (AOA).

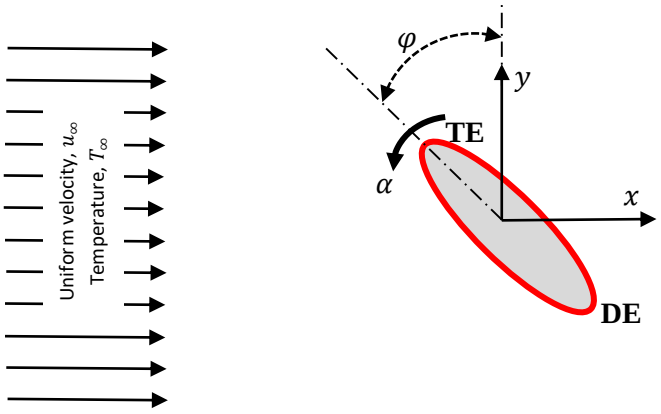

Figure 1. Schematic representation of the physical model.

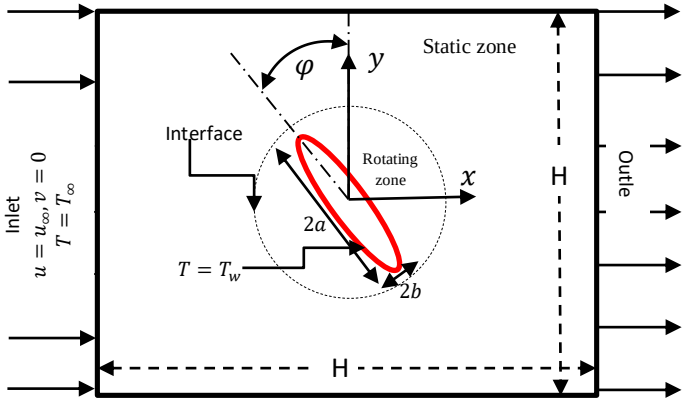

Figure 2. Schematic representation of the computational domain

Lua et al. [8] experimentally investigated the flow phenomenon around a two-dimensional elliptic airfoil rotating about its axis of symmetry in rested as well as flowing fluid. They show the presence of hovering vortex for the first time in parallel freestream. Naik et al. [9] numerically investigated the flow past rotating elliptic cylinder. They presented results for aspect ratio of the cylinder varies from 0.1 to 1, the non-dimensional rotational velocity of the cylinder from 0.5 to 1.5 and a single value of Reynolds number 100. They showed that the aspect ratio and rotation of the cylinder has a significant effect on the wake region and vortex shedding pattern. Recently Lua et al. [10] numerically investigated the rotating elliptic cylinder in a uniform cross flow. In their investigation, they varied the aspect ratio of the cylinder from 0.0625 to 1, the non-dimensional rotational speed of cylinder from 0 to 2.5 at constant Re = 200. Results show that a decreasing thickness generally leads to lower mean lift magnitude, but a non-monotonic change in mean drag with a local minimum at a thickness ratio of approximately 0.375. Paul et al. [11] numerically investigated the forced convection heat transfer from unconfined isothermal and isoflux elliptic cylinder. They varied the aspect ratio of the elliptic cylinder from 0.1 to 1 and show the variation of local and surface average Nusselt number with aspect ratio of the elliptic cylinder, AOA and Re. They concluded that the average Nu monotonically increases with aspect ratio (e) and Re, while Nu decreases with increasing value of AOA.

The objective of the present work is to study the influence of Prandtl and Reynolds number on local and average Nusselt number for a rotating elliptical cylinder. The aspect ratio and non-dimensional rotational speed of the elliptic cylinder (α) are considered 0.1 and 1 respectively. Reynolds number based on freestream velocity of the fluid ranges from $5 \leq Re \leq 40$ and Prandtl number is varying from 0.7 to 100.

PROBLEM STATEMENT AND GOVERNING EQUATIONS:

We consider a two-dimensional, laminar and steady flow of an incompressible fluid with a uniform velocity u_∞, and temperature T_∞ over an infinitely long (along z-direction) elliptic cylinder. The surface of the cylinder is kept the same at all instances of time. Also, the cylinder is made to rotate at constant angular speed in the counter-clockwise direction as shown schematically in Figure 1. We assume that the thermo-physical properties of the fluid are invariant with temperature and viscous dissipation of the fluid is also not significant. For justifying this assumption, the temperature difference between free-stream fluid and the surface of the cylinder is kept small. The continuity, momentum and energy equation in their dimensionless form can be written as

$$\frac{\partial U}{\partial X} + \frac{\partial V}{\partial Y} = 0, \tag{1}$$

$$\frac{\partial U}{\partial \tau} + \frac{\partial (UU)}{\partial X} + \frac{\partial (VU)}{\partial Y} = -\frac{\partial P}{\partial X} + \frac{1}{Re}\left(\frac{\partial^2 U}{\partial X^2} + \frac{\partial^2 U}{\partial Y^2}\right), \tag{2}$$

$$\frac{\partial V}{\partial \tau} + \frac{\partial (UV)}{\partial X} + \frac{\partial (VV)}{\partial Y} = -\frac{\partial P}{\partial Y} + \frac{1}{Re}\left(\frac{\partial^2 V}{\partial X^2} + \frac{\partial^2 V}{\partial Y^2}\right), \tag{3}$$

$$\frac{\partial T^*}{\partial \tau} + \frac{\partial (UT^*)}{\partial X} + \frac{\partial (VT^*)}{\partial Y} = \frac{1}{RePr}\left(\frac{\partial^2 T^*}{\partial X^2} + \frac{\partial^2 T^*}{\partial Y^2}\right). \tag{4}$$

where $Re = \frac{\rho u_\infty 2a}{\mu}$ and $Pr = \frac{\mu C_p}{K}$. Follwing scales are used to make governing equations non-dimensional

$$U = \frac{u}{u_\infty}, V = \frac{V}{u_\infty}, \tau = \frac{t u_\infty}{a}, X = \frac{x}{a}, Y = \frac{y}{a}$$

$$P = \frac{p}{\rho u_\infty^2}, T^* = \frac{T - T_\infty}{T_w - T_\infty}$$

The cylinder is placed in infinite medium but to make the problem solvable, we put artificial boundaries with appropriate boundary conditions. The computational domain is rectangular in shape (Fig. 2), and following boundary conditions are implemented over the confining boundaries

(1) Left boundary wall (inlet): uniform flow condition
$U = 1, V = 0, \frac{\partial P}{\partial X} = 0$ and $T^* = 0$

(2) Top and bottom boundary wall: free slip flow condition
$\frac{\partial U}{\partial Y} = 0, V = 0$ and $\frac{\partial T^*}{\partial Y} = 0$

(3) Right boundary wall: outflow condition
$\frac{\partial U}{\partial X} = 0, \frac{\partial V}{\partial X} = 0$ and $\frac{\partial T^*}{\partial X} = 0$

(4) At the solid surface of the cylinder:
$U = -\alpha \sin(\theta), V = -\alpha \cos(\theta), T^* = 1$

Using the computed flow and thermal fields local and global characteristics like drag and lift coefficients, stream function, and vorticity patterns, local and average Nusselt number are calculated.

NUMERICAL METHOD

The computational domain and grid are generated by using the commercial CFD software package ANSYS 15. The Governing differential equations solved using FLUENT. Due to the rotation of the cylinder, the solid-fluid boundary will change continuously, and the transient behaviour can be seen in the flow field. The moving fluid-solid boundary is resolved by Sliding Mesh Method (SMM). In this method, two mesh zones are created as shown schematically in Figure 2. The first mesh zone is circular in shape around the elliptic cylinder, and this zone is made to rotate at a speed of the cylinder. This zone is called as rotating mesh zone. The size of the cells inside this zone is kept small to accurately capture the unsteadiness behaviour of the flow around the cylinder. The rest of the region is stated as the stationary zone. The stationary and rotating zones are separated by a non-conformal interface. The interface of adjacent mesh zones is linked with one another and termed as a "mesh interface". The mesh zones move relative to each other along the mesh interface. Each moving zone's mesh is updated as a function of time. At each time interval, the computational domain has a new moving mesh form and the governing equations are solved at that instant of time.

RESULTS AND DISCUSSION

Before presenting the result, it is advisable to authenticate the numerical methodology executed in this problem. We first consider the flow around a heated rotating circular cylinder (can be assumed as an ellipse of aspect ratio $e = 1$) to validate our present results. Table 1 shows a comparison between the present and literature values for different values of Reynolds number (Re), Prandtl number (Pr), and non-dimensional rotational speed (α). A good agreement can be seen to exist between present and literature values.

Parameters					Values	
e	Re	α	AOA	Pr	Literature	Present
1	40	2	-	0.7	3.090 [2] 3.060 [3] 3.141 [1]	3.0322
1	5	2	-	0.7	1.4070 [1] 1.3817 [3]	1.3932
1	1	1	-	100	2.861 [4]	2.7900
0.1	50	-	30°	0.7	1.0621 [11]	1.0752

Table 1: Comparison of the present results with the literature values of Nusselt number

Flow patterns

In this section flow patterns in the vicinity of the elliptic cylinder are shown at four different orientations during rotation. The angle φ here is angle of the top edge with vertical. All the flow patterns presented in this section are shown after the flow has achieved a periodic state.

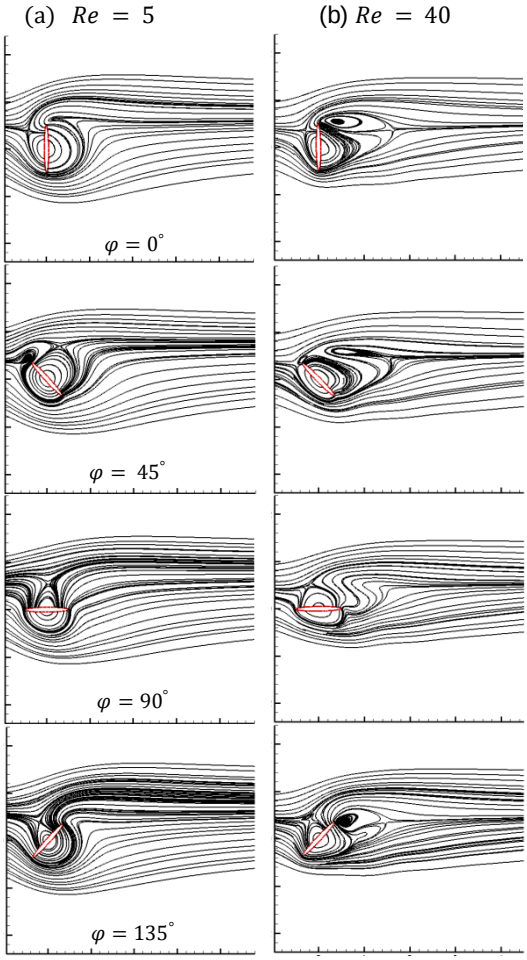

Figure 3: Streamline patterns near the cylinder for (a) Re = 5 and (b) Re =40.

The stable periodic state is confirmed by the time variation of drag and lift coefficients. When elliptic cylinder rotates, one tip moves in the direction of the freestream and the other tip

moves against the direction of the freestream. While discussing the results will mention the edge moving against the direction of the freestream as "Top edge" (TE) and edge moving in the direction of the fluid flow as "Down edge" (DE). Flow patterns are shown here (Fig. 3) are for extreme values of $Re = 5$ and 40. A detailed examination of the figure suggests that at low Reynolds number, flow is intact and no any kind of separation takes place at any instant of time during the rotation of the cylinder. As the Reynolds number increases flow start to separate near the top edge of the cylinder. This can be seen in Fig. 3(b) at all instant of time during the rotation of the cylinder except at the position when major axis of cylinder is parallel to the freestream direction i.e $\varphi = 90^{\circ}$. Increase in Reynolds number increase the tendency of wake formation behind the top edge and its size increases with Reynolds number. The flow pattern past the cylinder is same at $\varphi = 0^{\circ}$ and 180°, for all Re values due to the same orientation of the rotating cylinder. The only difference is that the top edge becomes down edge.

Isotherm patterns

In this section, the isotherm patterns around a rotating elliptic cylinder are presented for $Re = 5$ and 40 and $Pr = 1$ and 100. The isotherms shown here are again for stable periodic flow.

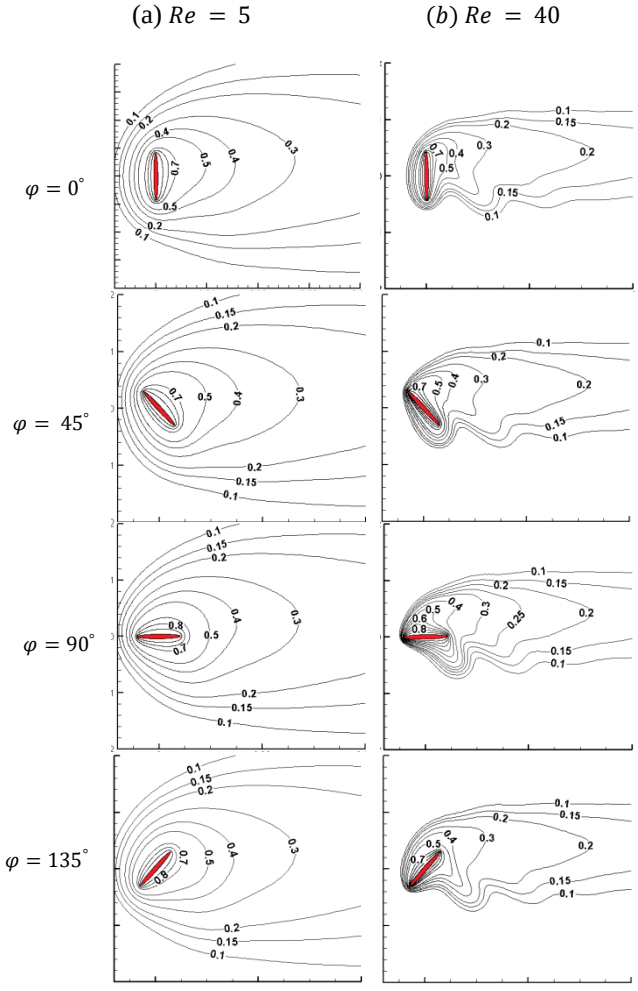

Figure 4: Isotherm profile at Pr = 1 and $(a)\ Re = 5$ & $(b)\ Re = 40$.

Figure 4 and 5 show representative isotherm profiles in the vicinity of the elliptic cylinder at four different instants of time. Figures show the influence of Prandtl number and Reynolds number on isotherms in the vicinity of the cylinder. The no of isotherms and levels are kept same in all figures to make a direct comparison. In Fig. 4(a) at lower Re the isotherms are widely spread around the cylinder however at high Re the spreading of isotherms are less. This is due to the thinner boundary layer (hydrodynamic and thermal both) at higher Reynolds number. The isotherm patterns around the cylinder for all four different orientations (Fig. 4(a)) at $Re = 5$ and $Pr = 1$ are very similar. Same conclusion can be drawn from the Fig. 4(b) at $Re = 40$ and $Pr = 1$ and Fig. 5(a) at $Re = 5$ and $Pr = 100$. The spreading of isotherms is remaining the same during the rotation. At low Peclet numbers ($Re \times Pr$), heat transfer happens predominantly by conduction process and consequently, the isotherms are not influenced by the rotation of the cylinder.

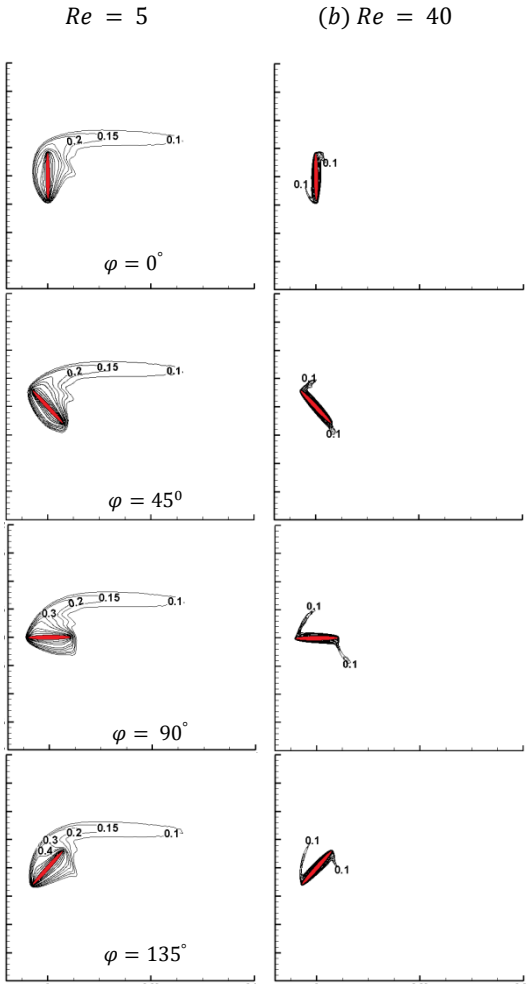

Figure 5: Isotherm profile at Pr = 100 and $(a)\ Re = 5$ & $(b)\ Re = 40$.

It can also be seen from the figures that the isotherms are more crowded at the top edge separation point which suggests the maximum value of the Nusselt number at that edge. The isotherms patterns at higher Prandtl number (Pr =100) are shown in figure 5(a) & 5(b). A detailed analysis of the figure suggests that with increment in Prandtl number, the thermal boundary layer becomes thinner which leads to an

increase in the temperature gradient in the vicinity of the cylinder. At higher Peclet number isotherms are confined near the cylinder which results into high temperature gradient thereby high Nusselt number.

Local Nusselt number

In this section, the distribution of Nusselt number on the surface of the cylinder is presented. In figures 6 and 7, the location $\theta = 0^0$ and 180^0 are positions of down edge and top edge, respectively. Figure 6 shows the variation of local Nusselt number with θ position at four different orientations of the cylinder. For all orientations, Local Nusselt number is not changing significantly except near top and down edge. This is seen for all values of Re and Pr considered here. Figure 7 shows the variation of local Nusselt number at different Prandtl numbers. The variation shown here is for $\varphi = 90$ and extreme values of $Re = 5$ and 40. This particular orientation is considered here because at this position average Nusselt number shows maximum value. As expected the local Nusselt numbe is seen to increase with Prandtl number and Reynolds number.

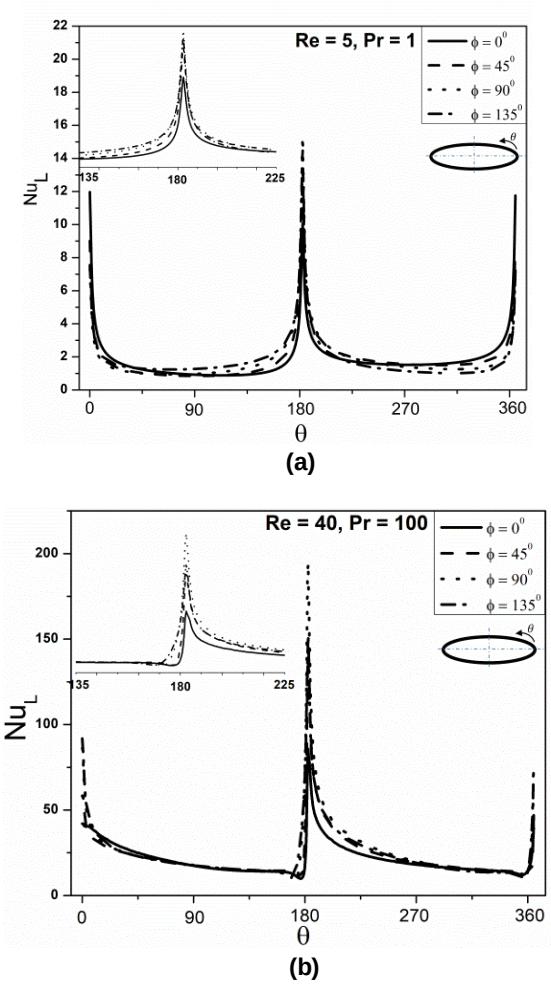

Figure 6: Variation of local Nusselt number over the rotating cylinder surface with its orientation at (a) $Re = 5$ and $Pr = 1$ and (b) $Re = 40$ and $Pr = 100$.

Average Nusselt number

The surface average values are frequently desirable for process design calculation. As literature suggests, the average Nusselt number is expected to be a function of Re number and Pr number. The plot shown in Fig. 8 highlights the effect of each of these parameters. A detailed assessment of Figure 8 reveals that on increasing the value of the Reynolds number, for the fixed values of the Prandtl number, the value of the average Nusselt increases.

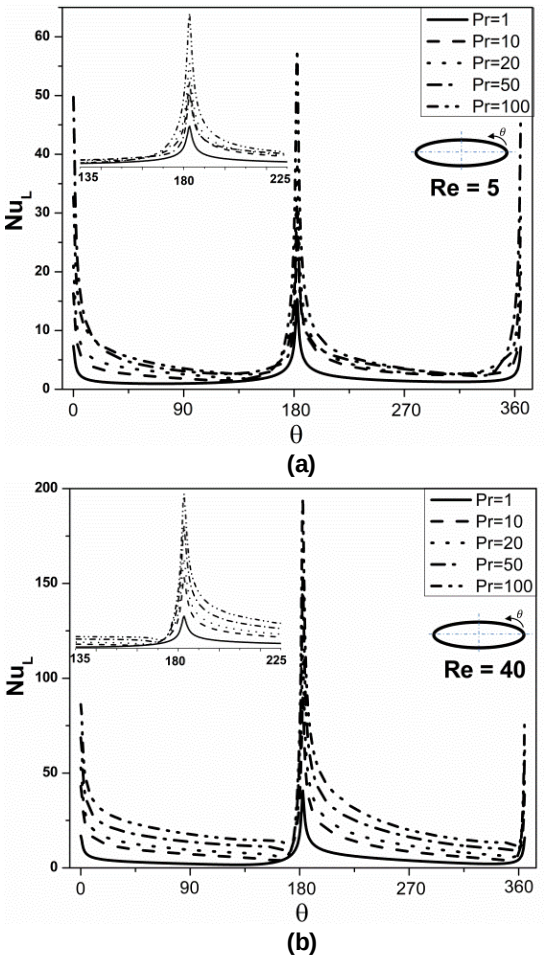

Figure 7: Variation of local Nusselt number with Prandtl number at (a) $Re = 5$ and (b) $Re = 40$.

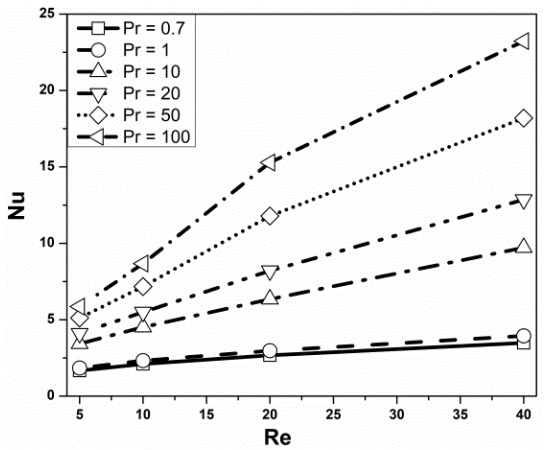

Figure 8: Variation of surface average Nusselt number with Prandtl number and Reynolds number.

For the fixed value of the Reynolds number, the value of average Nusselt number increases with increment in Prandtl number. This can be explained as with increment in Prandtl number the momentum diffusivity dominant over thermal diffusivity thereby thinning the thermal boundary layer and enhancement of heat transfer. This can be also explained from the figure that increment in Nu is more at higher Re and Pr as compare to lower Re and Pr.

Conclusions

In this study, the effect of Prandtl number on forced convective heat transfer from a heated elliptic cylinder of aspect ratio ($e = 0.1$) rotating in flowing fluid have been numerically investigated. Numerical computations are performed for the ranges of conditions: $5 \leq Re \leq 40$; $1 \leq Pr \leq 100$; $\alpha = 1$. The flow patterns, isotherm patterns, local Nusselt number and surface averaged Nusselt number are presented and examined for the range of conditions. In the considering range, for the fixed value of the Re, the value of the surface average and local Nusselt number increases with increasing value of Prandtl number. It is also seen that isotherm patterns and local Nusselt number are not much affected by the orientation of the rotating cylinder.

References

1. H. M. Badr, and S. C. R. Dennis. 1985. "Laminar Forced Convection from a Rotating Cylinder." *International Journal of Heat and Mass Transfer*, 28(1): 253-264. doi: 10.1016/0017-9310(85)90027-4.
2. Sachin B. Paramane, and Atul Sharma. 2009. "Numerical Investigation of Heat and Fluid Flow Across a Rotating Circular Cylinder Maintained at Constant Temperature in 2-D Laminar Flow Regime." *International Journal of Heat and Mass Transfer* 52(13-14): 3205-3216. doi: 10.1016/j.ijheatmasstransfer.2008.12.031.
3. Saroj K. Panda and R. P. Chhabra. 2011. "Laminar Forced Convection Heat Transfer from a Rotating Cylinder to Power-Law Fluids." *Numerical Heat Transfer, Part A: Applications* 59(4): 297-319. doi:10.1080/10407782.2011.549369
4. V. Sharma, and K. Dhiman. 2012. "Heat Transfer From a Rotating Circular Cylinder in the Steady Regime: Effects of Prandtl number". *Thermal Science*, 16(1): 79–91. doi:10.2298/tsci100914057s
5. Z. Li, J.H. Davidson, and S.C. Mantell. 2005. "Numerical Simulation of Flow Field and Heat Transfer of Streamlined Cylinders in Cross Flow." *ASME. J. Heat Transfer* 128(6): 564-570. doi:10.1115/1.2188463.
6. Ota Terukazu, Aiba Shinya, Tsuruta Tsunehiko and Kaga Masaaki. 1983. "Forced Convection Heat Transfer From on Elliptic Cylinder of Axis Ratio 1: 2." *Bulletin of JSME* 26: 262-267. doi:10.1299/jsme1958.26.262.
7. Ota Terukazu, Hideya Nishiyama and Taoka Yukiyasu. 1984. "Heat Transfer and Flow around an Elliptic Cylinder." *International Journal of Heat and Mass Transfer* 27: 1771-1779. doi:10.1016/0017-9310(84)90159-5.
8. Kim Boon Lua, T. T. Lim, and K. Yeo. 2010. "A Rotating Elliptic Airfoil in Fluid at Rest and in a Parallel Freestream." *Experiments in Fluids* 49: 1065-1084. doi:10.1007/s00348-010-0847-7.
9. Sandeep N. Naik, S. Vengadesan, and K. Arul Prakash. 2017. "Numerical study of fluid flow past a rotating elliptic cylinder." *Journal of Fluids and Structures* 68: 15-31. doi:10.1016/j.jfluidstructs.2016.09.011.
10. Kim Boon Lua, Hao Lu, and T.T. Lim. 2017. "Rotating Elliptic Cylinders in a Uniform Cross Flow". *Journal of Fluids and Structures* 78: 36-51. doi:10.1016/j.jfluidstructs.2017.12.023.
11. Immanuvel Paul, K. Arul Prakash and S. Vengadesan. 2013. "Forced Convective Heat Transfer from Unconfined Isothermal and Isoflux Elliptic Cylinders." *Numerical Heat Transfer, Part A: Applications* 64 (8): 648-675. doi:10.1080/10407782.2013.790261